



Direct probing of acylperoxy radicals during ozonolysis of α -pinene: constraints on radical chemistry and production of highly oxygenated organic molecules

Han Zang¹, Dandan Huang², Jiali Zhong³, Ziyue Li¹, Chenxi Li¹, Huayun Xiao¹, and Yue Zhao¹

¹School of Environmental Science and Engineering, Shanghai Jiao Tong University, Shanghai, 200240, China

²Shanghai Academy of Environmental Sciences, Shanghai, 200233, China

³Division of Environment and Sustainability, Hong Kong University of Science and Technology, Hong Kong SAR, 999077, China

Correspondence: Yue Zhao (yuezhao20@sjtu.edu.cn)

Received: 26 April 2023 – Discussion started: 15 May 2023

Revised: 28 August 2023 – Accepted: 31 August 2023 – Published: 11 October 2023

Abstract. Acylperoxy radicals (RO_2) are key intermediates in the atmospheric oxidation of organic compounds and different from the general alkyl RO_2 radicals in reactivity. However, direct probing of the molecular identities and chemistry of acyl RO_2 remains quite limited. Here, we report a combined experimental and kinetic modeling study of the composition and formation mechanisms of acyl RO_2 , as well as their contributions to the formation of highly oxygenated organic molecules (HOMs) during ozonolysis of α -pinene. We find that acyl RO_2 radicals account for 67 %, 94 %, and 32 % of the highly oxygenated C_7 , C_8 , and C_9 RO_2 , respectively, but only a few percent of C_{10} RO_2 . The formation pathway of acyl RO_2 species depends on their oxygenation level. The highly oxygenated acyl RO_2 (oxygen atom number ≥ 6) are mainly formed by the intramolecular aldehydic H shift (i.e., autoxidation) of RO_2 , while the less oxygenated acyl RO_2 (oxygen atom number < 6) are basically derived from the C–C bond cleavage of alkoxy (RO) radicals containing an α -ketone group or the intramolecular H shift of RO containing an aldehyde group. The acyl- RO_2 -involved reactions explain 50 %–90 % of C_7 and C_8 closed-shell HOMs and 14 % of C_{10} HOMs, respectively. For C_9 HOMs, this contribution can be up to 30 %–60 %. In addition, acyl RO_2 contribute to 50 %–95 % of C_{14} – C_{18} HOM dimer formation. Because of the generally fast reaction kinetics of acyl RO_2 , the acyl RO_2 + alkyl RO_2 reactions seem to outcompete the alkyl RO_2 + alkyl RO_2 pathways, thereby affecting the fate of alkyl RO_2 and HOM formation. Our study sheds lights on the detailed formation pathways of the monoterpene-derived acyl RO_2 and their contributions to HOM formation, which will help to understand the oxidation chemistry of monoterpenes and sources of low-volatility organic compounds capable of driving particle formation and growth in the atmosphere.

1 Introduction

Monoterpenes ($\text{C}_{10}\text{H}_{16}$) comprise an important fraction of nonmethane hydrocarbons in the global atmosphere (Guenther et al., 2012; Sindelarova et al., 2014) and make a significant contribution to the secondary organic aerosol (SOA) budget (Pye et al., 2010; Iyer et al., 2021). The presence of a double bond and the large molecular size of monoterpenes favor their oxidation reactivity towards O_3 , hydroxyl (OH), and nitrate (NO_3) radicals (Atkinson et al., 1990, 1986; Kurten

et al., 2015; Kristensen et al., 2016; Bianchi et al., 2019; Berndt, 2022), as well as the formation of low-volatility products and SOA (Fry et al., 2009, 2014; Zhang et al., 2018; Bianchi et al., 2019; Molteni et al., 2019; Shen et al., 2022). The organic peroxy radicals (RO_2) in the gas-phase oxidation of monoterpenes can undergo autoxidation and form a class of highly oxygenated organic molecules (HOMs) (Jokinen et al., 2014; Mentel et al., 2015; Berndt et al., 2016; Zhao et al., 2018; Bianchi et al., 2019; Bell et al., 2022; Berndt, 2022), which are primarily low-volatility or extremely low-

volatility organic compounds (LVOCs and ELVOCs) (Ehn et al., 2014; Bianchi et al., 2019) and thus play a crucial role in SOA formation and growth.

Significant advances have been made in recent years concerning the monoterpene RO₂ autoxidation and its contribution to HOM formation (Ehn et al., 2014; Berndt et al., 2016; Zhao et al., 2018; Xu et al., 2019; Lin et al., 2021; Berndt, 2022; Shen et al., 2022). It is recognized that some monoterpene RO₂ radicals derived from the traditional ozonolysis channel (i.e., isomerization of Criegee intermediates, CIs) and OH addition channel can autoxidize at a rate larger than 1 s⁻¹ and could be an important contributor to HOM formation (Zhao et al., 2018; Xu et al., 2019; Berndt, 2021). Recently, new reaction channels leading to the RO₂ radicals that can undergo fast autoxidation have been proposed. A quantum chemical calculation study indicated that an excited CI arising from α -pinene ozonolysis could undergo ring-breaking reactions and directly lead to a ring-opened RO₂ due to the excess energy, which can autoxidize at a rate of ~ 1 s⁻¹ and rapidly form highly oxidized RO₂ with up to 8 oxygen atoms (Iyer et al., 2021). In addition, the minor hydrogen abstraction channel by OH radicals has been proposed as a predominant pathway to HOM formation from OH oxidation of α -pinene under atmospheric conditions (Shen et al., 2022).

RO₂ species can be simply divided into alkyl RO₂ and acyl RO₂ (RC(O)OO) according to whether R is an acyl radical. There are significant differences in the reactivity of these two kinds of RO₂. Firstly, the rate constant of acyl RO₂ with NO is in general slightly higher than that of alkyl RO₂ (Atkinson et al., 2007; Calvert et al., 2008; Orlando and Tyndall, 2012). For example, the reaction rate constants of acyl RO₂, CH₃C(O)O₂, and alkyl RO₂, CH₃CH₂O₂, with NO have been reported to be 20×10^{-12} and 9.2×10^{-12} cm³ molec.⁻¹ s⁻¹, respectively (Atkinson et al., 2007; Calvert et al., 2008; Orlando and Tyndall, 2012). Besides, acyl RO₂ can react rapidly with NO₂ and form thermally unstable peroxyacyl nitrates (RC(O)OONO₂), which have a lifetime of tens of minutes at room temperature and of days and even months in winter or in the upper atmosphere with lower temperatures (Atkinson et al., 2007; Orlando and Tyndall, 2012). Although alkyl RO₂ radicals can also react with NO₂ and form the alkyl peroxy nitrates (ROONO₂), they are extremely unstable and will decompose into RO₂ radicals and NO₂ in less than 1 s (Kirchner et al., 1997; Orlando and Tyndall, 2012). Lastly, the rate constant of cross-reaction of acyl RO₂ ($1.5 \pm 0.3 \times 10^{-11}$ cm³ molec.⁻¹ s⁻¹) is significantly higher than that of alkyl RO₂ (2×10^{-17} – 1×10^{-11} cm³ molec.⁻¹ s⁻¹) (Villenave and Lesclaux, 1996; Tyndall et al., 2001; Atkinson et al., 2007; Zhao et al., 2018). As a result, these two kinds of RO₂ may play different roles in the autoxidation as well as HOM and dimer formation.

The quantum calculations revealed that different functional groups in RO₂ would lead to significantly different intramolecular H-shift rates (Otkjær et al., 2018). The C=O

and C=C substituents led to resonance-stabilized carbon radicals and could enhance the H-shift rate constants by more than a factor of 400. The fast aldehydic H-shift rate contributes to a series of acyl radicals (RC(O)) with the radical site at the terminal carbonyl carbon, which further produce the acyl RO₂ with O₂ addition. Many RO₂ formed in the oxidation of monoterpenes have the aldehyde functionality, especially for α -pinene ozonolysis, in which all the primary and many later-generation RO₂ contain at least one aldehyde group (Noziere et al., 2015; Berndt et al., 2018; Li et al., 2019; Berndt, 2022; Zhao et al., 2022). As a result, acyl RO₂ may comprise a considerable fraction of total RO₂ species and contribute significantly to the formation of low-volatility products and SOA in the monoterpene oxidation system. A recent study by Zhao et al. (2022) found that the acyl-RO₂-involved reactions contribute to 50%–80% of oxygenated C₁₅–C₂₀ dimers (O : C ≥ 0.4) and 70% of C₁₅–C₁₉ dimer esters in SOA from α -pinene ozonolysis. However, currently the direct probing of the molecular identities and chemistry of monoterpene-derived acyl RO₂ radicals is rather limited. The role of acyl RO₂ in HOM formation remains to be quantified.

In this study, the molecular identities and formation mechanisms of acyl RO₂ radicals, as well as their contributions to HOM formation in the α -pinene ozonolysis, are investigated. The experiments were conducted in a flow reactor with different concentrations of NO₂, which acted as an efficient scavenger for the acyl RO₂. The molecular composition and abundance of the gas-phase HOMs were measured by a chemical ionization–atmospheric pressure interface–time-of-flight mass spectrometer (CI-API-ToF) using nitrate as the reagent ions. In addition, kinetic modeling using the Framework for 0-D Atmospheric Modeling (FOAM v4.1) employing the Master Chemical Mechanism (MCM v3.3.1), updated with the latest advances of the RO₂ chemistry, was performed to gain insights into the reaction kinetics and mechanisms of acyl RO₂ species. We find that acyl RO₂ account for a major fraction of highly oxygenated C₇ and C₈ RO₂ and play a significant role in the formation of HOM monomers and dimers with small molecular size. This study will help to understand the role of acyl RO₂ in the formation of low-volatility species from monoterpene oxidation and reduce the uncertainties in the future atmospheric modeling of the formation and impacts of aerosols.

2 Method and materials

2.1 Flow reactor experiments

The α -pinene ozonolysis experiments were carried out under room temperature (298 K) and dry conditions (relative humidity < 5%) in a custom-built flow reactor, which has been described in detail previously (Yao et al., 2019). The α -pinene vapor was generated by evaporating its pure liquid (99%, Sigma-Aldrich) into a flow of zero air

(10.65 L min⁻¹) added to the reactor using an automated syringe pump (TYD01–01 CE, Baoding Leifu Fluid Technology Co., Ltd.). The initial concentrations of α -pinene ranged from 500 ppb to 3 ppm in different experiments. Ozone was generated by passing a flow of ultra-high-purity (UHP) O₂ (150 mL min⁻¹, Shanghai Maytor Special Gas Co., Ltd.) through a quartz tube housing a pen-ray mercury lamp (UV-S2, UVP Inc.), and its concentration (45 and 180 ppb under low and high O₃ conditions, respectively) was measured by an ozone analyzer (Model 49i, Thermo Fisher Scientific, USA). The NO₂, acting as an acyl RO₂ scavenger, was derived from its standard cylinder gas (15.6 ppm, Shanghai Weichuang Standard Gas Co., Ltd.), and its initial concentration ranged from 0 to 30 ppb. To validate the formation mechanisms of acyl RO₂, selected experiments with the addition of NO or cyclohexane were also conducted. NO was derived by its standard cylinder gas (9.8 ppm, Shanghai Weichuang Standard Gas Co., Ltd.), and its initial concentration also ranged from 0 to 30 ppb. The gas-phase cyclohexane (~ 500 ppm), acting as an OH scavenger, was generated by bubbling a gentle flow of UHP N₂ through liquid cyclohexane (LC-MS grade, CNW). The total air flow in the flow reactor was 10.8 L min⁻¹, and the residence time was 25 s. The relatively low O₃ concentration and short reaction time in the flow reactor avoid significant production of NO₃ radicals from NO₂ and O₃ and make the NO₃ oxidation contribute only 0.3 %–1.2 % of the total α -pinene oxidation in our experiments. Therefore, the NO₃ chemistry could be neglected in this study. A summary of the experimental conditions is given in Tables S1 and S2 in the Supplement.

The gas-phase RO₂ radicals and closed-shell products were measured by a nitrate-based CI-API-ToF mass spectrometer (abbreviated as nitrate-CIMS; Aerodyne Research, Inc.), and a long time-of-flight mass spectrometer with a mass resolution of ~ 10 000 Th/Th was used here. The mass calibration error is below 1.8 ppm. The sheath flow, including a 2 mL min⁻¹ UHP N₂ flow containing nitric acid (HNO₃) and 22.4 L min⁻¹ zero air, was guided through the PhotoIonizer (Model L9491, Hamamatsu, Japan) to generate nitrate reagent ions. The total sample flow rate was 9 L min⁻¹ during the experiments. The mass spectra within the m/z range of 50 to 700 were analyzed using the tofTools package developed by Junninen et al. (2010) based on MATLAB.

To clarify whether there is SOA formation in the experiments, a scanning mobility particle sizer (SMPS, TSI), which consists of an electrostatic classifier (model 3082), a long or nano differential mobility analyzer (model 3081 and 3085 for different particle sizes), and a condensation particle counter (model 3756), was used to monitor the formation of SOA particles. Except in Experiment (Exp) 31 where the reacted α -pinene reached 36.8 ppb and there was low SOA formation with particle mass concentrations of 5.0×10^{-4} – 5.7×10^{-3} $\mu\text{g m}^{-3}$ and number concentrations of 63–395 cm⁻³, no particle formation was observed by SMPS. Therefore, the RO₂ radicals and closed-shell products would

be primarily distributed in the gas phase, with their fates negligibly influenced by the low SOA formation under these experimental conditions.

2.2 Kinetic model simulations

Model simulations of RO₂ and HOM formation in selected experiments were performed to constrain the reaction kinetics and mechanisms of acyl RO₂ using FOAM v4.1 (Wolfe et al., 2016), which employs MCM v3.3.1 (Jenkin et al., 2015) updated with the chemistry of RO₂ autoxidation and cross-reactions forming HOM monomers and dimers. Newly added species and reactions to MCM v3.3.1 followed the work by Zhao et al. (2018) and Wang et al. (2021). Considering that the default MCM v3.3.1 does not include highly oxygenated acyl RO₂, we added the possible formation pathways of the potential acyl RO₂ measured in this study to the model based on the mechanisms proposed by Zhao et al. (2022).

The formation and reaction branching ratios of the two α -pinene-derived CIs are updated in the model according to the recent studies (Table S3) (Claffin et al., 2018; Iyer et al., 2021; Zhao et al., 2021; Berndt, 2022). The formation of a ring-opened C₁₀H₁₅O₄-RO₂ species (C10H15O4RBRO2 in Table S3) from α -pinene ozonolysis proposed by a recent study (Iyer et al., 2021), as well as its subsequent autoxidation and bimolecular reactions, is included in the model. The autoxidation rate constant of the ring-opened C₁₀H₁₅O₄-RO₂ is 1 s⁻¹, and a lower limit of its molar yield (30 %) was used according to the recent studies (Zhao et al., 2021; Meder et al., 2023) and our results (see details in Sect. 3.3). We also added the hydrogen abstraction channel of α -pinene oxidation by OH radicals according to a recent study (Shen et al., 2022). The branching ratio of this channel was set to 9 %, with the remaining 91 % being the traditional OH addition pathways. The detailed reaction pathways and rate constants of RO₂ species in this channel followed the work by Shen et al. (2022), except for RO₂ cross-reactions, the rates of which were not reported in that study. As the primary RO₂ radicals (C₁₀H₁₅O₂-RO₂) formed via the hydrogen abstraction by OH radicals are least oxidized with only 2 oxygen atoms, their cross-reaction rate could be relatively low (Atkinson et al., 2007; Orlando and Tyndall, 2012). In the model, this rate constant was set to 1×10^{-13} cm³ molec.⁻¹ s⁻¹. For other alkyl RO₂ radicals (including HOM-RO₂), their cross-reaction rate constant is assumed to be 1×10^{-12} cm³ molec.⁻¹ s⁻¹ according to Zhao et al. (2018). The dimer formation rates for these alkyl RO₂ are same as their cross-reaction rates.

In flow reactor experiments, the equilibrium formation of ROONO₂ would lead to the consumption of alkyl RO₂ radicals. To account for the influence of this process on the RO₂ budget and HOM formation, we included the reaction of RO₂ + NO₂ \rightleftharpoons ROONO₂ in the model, with forward and reverse reaction rate constants of 7.5×10^{-12} cm³ molec.⁻¹ s⁻¹ and 5 s⁻¹, respectively (Orlando and Tyndall, 2012). To sim-

plify the parameterization, the forward and reverse reaction rate constants of newly added highly oxygenated acyl RO₂ with NO₂ are the same as default values in MCM v3.3.1. Besides, the cross-reaction rate constants of acyl RO₂ (including acyl RO₂ + acyl RO₂ and acyl RO₂ + alkyl RO₂) forming monomers or dimers were both set to $1 \times 10^{-11} \text{ cm}^3 \text{ molec.}^{-1} \text{ s}^{-1}$ (Orlando and Tyndall, 2012). Considering that there are large uncertainties in the dimer formation rate of RO₂, a sensitivity analysis was conducted to evaluate its influence on acyl-RO₂-involved HOM formation by varying the rate constant from 1×10^{-13} to $1 \times 10^{-12} \text{ cm}^3 \text{ molec.}^{-1} \text{ s}^{-1}$ for alkyl RO₂ and 1×10^{-12} to $1 \times 10^{-11} \text{ cm}^3 \text{ molec.}^{-1} \text{ s}^{-1}$ for acyl RO₂. The results show that changes in dimer formation rate constants within the above ranges have no significant influence on the contribution of acyl RO₂ to HOM formation (Fig. S1 in the Supplement).

The wall losses of OH, HO₂, and RO₂ radicals, as well as closed-shell HOM monomers and dimers in the flow reactor, were considered using the Knopf–Pöschl–Shiraiwa (KPS) method proposed by Knopf et al. (2015) in the model (Table S4), with an assumption of irreversible uptake of these species on the reactor wall. It is found that the wall loss of OH, HO₂, and RO₂ radicals accounts for 0.08%–0.14%, 4.7%–9.1%, and 7.3%–25.5% of their total production, respectively, with lower values under higher reacted α -pinene concentration conditions. Therefore, the wall loss process would not significantly influence α -pinene oxidation and RO₂ chemistry. The wall losses of closed-shell HOM monomers and dimers account for 18.4%–34.7% and 14.2%–33.1% of their total production, respectively. It should be noted that the wall losses of typical RO₂ and HOMs have a negligible impact on their responses to the addition of NO₂ (Fig. S2). In addition, with the consideration of the wall loss effects, the contribution of acyl RO₂ to the HOM formation only changed a little (0.02%–0.5%). Therefore, the wall losses of RO₂ and HOMs in the flow reactor would not affect the interpretation of the results in this study.

3 Results and discussion

3.1 Molecular composition of acyl RO₂ from α -pinene ozonolysis

The overall formation characteristics of gas-phase RO₂, closed-shell monomers, and dimers with the addition of NO₂ (30 ppb) are shown in Fig. 1 (Exps 8 and 14, Table S1). Since the nitrate-CIMS is only highly sensitive to the highly oxygenated species, we only discuss the production of HOMs with oxygen atoms above 6 here. As for RO₂ and closed-shell monomers (Fig. 1a), the signals of C₇ and C₈ species decrease by more than 50% with the addition of NO₂, while for C₉ and C₁₀ species, their decreases are relatively small (within 40%). In addition, we note that there is an unexpected increase in some C₉ and C₁₀ RO₂, and the possible reason will be discussed in detail later.

NO₂ could react rapidly with acyl RO₂ radicals to form RC(O)OONO₂, which has a higher thermal-stability compared to ROONO₂ and can serve as a sink for acyl RO₂ on our experimental timescales. Therefore, a significant decrease in C₇ and C₈ RO₂ and HOMs upon the addition of NO₂ indicates that a major fraction of C₇ and C₈ RO₂ are acyl RO₂. In contrast, the slight decrease in C₉ and C₁₀ HOM monomers shows that the contribution of acyl RO₂ to C₉ and C₁₀ RO₂ is relatively small. However, some of the C₁₀ monomers showed a slight increase with the addition of NO₂, especially for C₁₀H₁₈O_x HOMs. The addition of NO₂ plays a twofold role in dimer formation from α -pinene ozonolysis (Fig. 1b). There is a significant inhibiting effect on C₁₄–C₁₈ dimers, which is due to the large contribution of acyl RO₂ to the total C₇ and C₈ RO₂ that generate such dimers. However, C₁₉ and C₂₀ dimers only show a slight decrease with the addition of NO₂, and some of them are even enhanced. In particular, the enhancement in C₂₀H₃₄O_x is most significant, reaching 30%.

Kinetic model simulations show that the concentration of alkyl RO₂ decreases by 1%–20% with the addition of 30 ppb NO₂ under different reacted α -pinene conditions (Exps 1–28). Considering that the acyl RO₂ could be rapidly consumed by NO₂, if the signal reduction of a RO₂ specie significantly exceeds 20% with 30 ppb NO₂ addition, we presume it has significant contribution from acyl RO₂. As a result, a total of 10 acyl RO₂ were identified according to the changes of RO₂ signal as a function of initial NO₂ concentration, which include C₇H₉O₆, C₇H₉O₇, C₈H₁₃O₆, C₈H₁₃O₈, C₈H₁₃O₉, C₈H₁₃O₁₀, C₉H₁₃O₉, C₉H₁₇O₇, C₉H₁₇O₉, and C₁₀H₁₅O₇. Figure 2 shows the averaged normalized acyl RO₂ signals measured as a function of the added NO₂ concentration under different experimental conditions (Exps 1–28). Similarly, since the nitrate-CIMS is only highly sensitive to products with high oxygen content, we only observed acyl RO₂ with oxygen atoms above 6. Consistent with the significant decrease in C₇ and C₈ species with the addition of NO₂ in Fig. 1a, C₇ and C₈ acyl RO₂ decrease by more than 50% with the increase in NO₂ concentration (Fig. 2a and b). For C₉ acyl RO₂, the C₉H₁₇O₇-RO₂ and C₉H₁₇O₉-RO₂ also decrease dramatically with increasing NO₂, and the decrease in C₉H₁₃O₉-RO₂ is relatively smaller (Fig. 2c). In addition, C₁₀H₁₅O₇-RO₂ also shows a small decrease (Fig. 2d), with a reduction of only 30% at 30 ppb NO₂. The relatively small reduction in the abundance of some of these RO₂ radicals indicates the presence of alkyl RO₂ radicals with the same chemical formulas. Along with the marked reduction in acyl RO₂ signals, the production of highly oxygenated RC(O)OONO₂ species such as C₉H₁₃O₉NO₂, C₉H₁₇O₇NO₂, and C₁₀H₁₅O₇NO₂ with the addition of NO₂ was observed (see the spectra in Fig. S3). However, we note that although some RC(O)OONO₂ such as C₈H₁₃O₆NO₂ and C₈H₁₃O₈NO₂ are expected to be formed with NO₂ addition, they could not be unambiguously detected by the nitrate-CIMS due to the overlapping of their peaks with

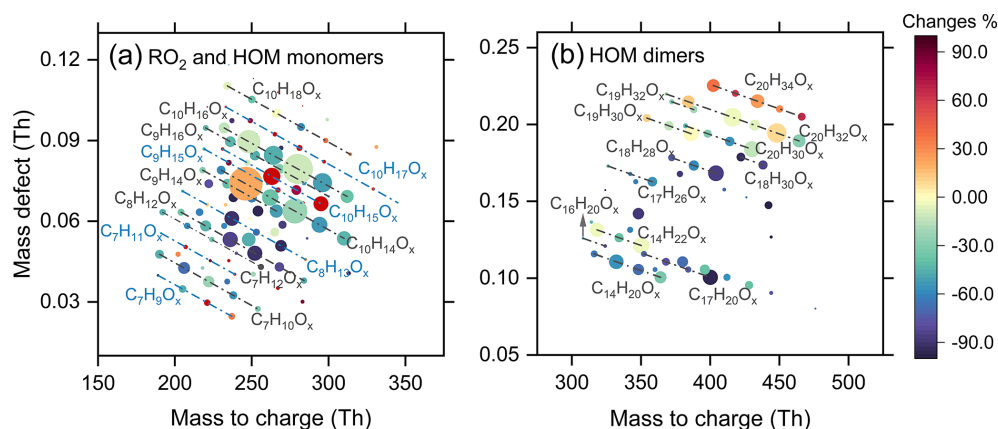


Figure 1. Mass defect plots of (a) RO₂ and HOM monomers and (b) HOM dimers formed from ozonolysis of α -pinene in the presence of NO₂ measured using a nitrate-CIMS (Exps 8, 14). The circles are colored by the relative changes in signal of RO₂, monomers, and dimers due to the addition of NO₂ (30 ppb). The area of circles is linearly scaled with the cube root of the signal of HOMs formed in the absence of NO₂. The blue lines represent RO₂ radicals.

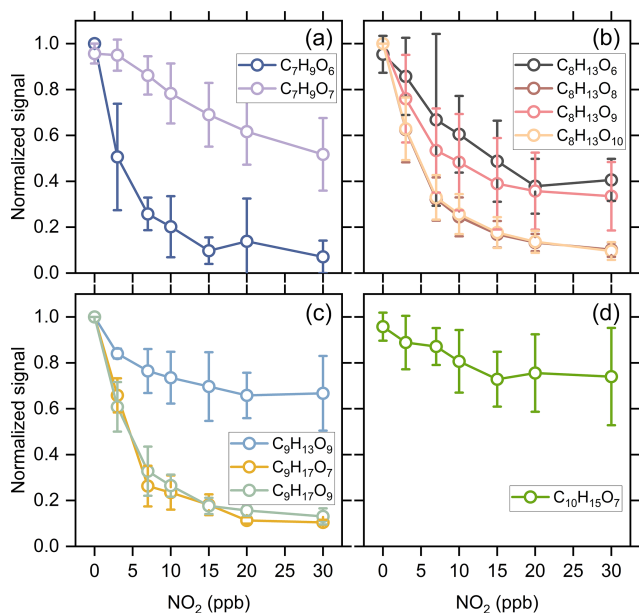


Figure 2. Averaged normalized signal of the measured acyl RO₂ as a function of the added NO₂ concentration under different experimental conditions (Exps 1–28).

strong alkyl RO₂ peaks (C₉H₁₅O₈-RO₂ and C₉H₁₅O₁₀-RO₂) in this study.

Figure 3 shows the contribution of acyl and alkyl RO₂ to the highly oxygenated C₇–C₁₀ RO₂. Acyl RO₂ contribute 66.9%, 94.3% and 31.7% to the total C₇, C₈, and C₉ RO₂ signals, respectively. By contrast, the only C₁₀ acyl RO₂ measured in this study is C₁₀H₁₅O₇, which contributes to only 0.4% of the total C₁₀ RO₂. It should be noted that there might be other C₁₀ acyl RO₂ that were not observed due to the interferences from the alkyl RO₂ with the same chemical

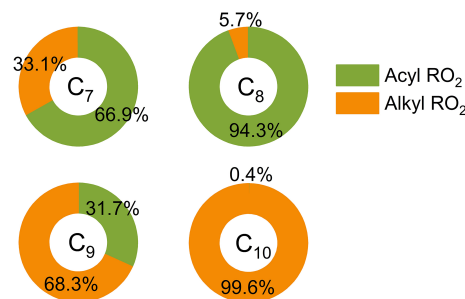


Figure 3. Contributions of acyl and alkyl RO₂ to the highly oxygenated C₇–C₁₀ RO₂ measured by a nitrate-CIMS.

formulas, which respond differently to the addition of NO₂ than acyl RO₂ do (see details in the following discussion). Considering that some RO₂ formulas such as C₁₀H₁₅O₇ may have contributions from both acyl RO₂ and alkyl RO₂, we assumed the decrease of RO₂ signal with the addition of NO₂ as the signal of acyl RO₂. Besides, it is obvious that the normalized signal basically decreases to the lowest value when the initial NO₂ concentration reaches 10 ppb (Fig. 2), indicating that most of the acyl RO₂ are depleted at this NO₂ concentration. In addition, the decreasing extents of some acyl RO₂ are different for different reacted α -pinene concentrations, with lower decreasing extent for higher reacted α -pinene concentrations (Fig. S4). This difference might be due to the promoted cross-reactions of acyl RO₂ as well as their precursor RO₂ at higher α -pinene concentrations, which are competitive with the reactions leading to acyl RO₂ formation as well as the acyl RO₂ + NO₂ reactions.

In addition to the changes of acyl RO₂ signal, we also show the changes of normalized alkyl RO₂ signal with the increasing initial NO₂ concentration in Fig. S5. Although ROONO₂ formed by the reaction of alkyl RO₂ with NO₂ is

thermally unstable and would decompose quickly to release RO₂, it would still reach a formation–decomposition equilibrium in the system, thus consuming a small amount of alkyl RO₂. However, it can be seen from Fig. S5 that during 25 s of reaction in the flow reactor, a large part of alkyl RO₂ has an increasing trend with the increase in NO₂ concentration. We speculate that a portion of ROONO₂ could decompose back to RO₂ and NO₂ in the nitrate chemical ionization inlet where the sample gases were diluted instantly and the equilibrium of ROONO₂ was disturbed, resulting in the release of a large amount of RO₂.

To verify our speculation, the decomposition of ROONO₂ in the chemical ionization inlet was simulated based on the dilution ratio (1 : 3.5) and residence time (200 ms) in the inlet. As shown in Fig. S6, more than 40 % of ROONO₂ decomposes back to RO₂ and NO₂ in the chemical ionization inlet, which would inevitably lead to an increase in RO₂ concentration. As the C₁₀H₁₅O₈NO₂ has a significant contribution from the relatively stable RC(O)OONO₂ arising from the ring-opened acyl C₁₀H₁₅O₈-RO₂ reported by Iyer et al. (2021), its decomposition is relatively small (~ 21 %). It should be noted that the RO₂ measured here is only a part of total RO₂ produced and that a large amount of RO₂ has already reacted to form closed-shell products as well as ROONO₂ in the flow reactor. Taking Exp 14 as an example (30 ppb NO₂), the simulated concentrations of RO₂ and ROONO₂ are 1.3 and 1.9 ppb, which approximately accounts for 27.1 % and 39.6 % of the total production of RO₂, respectively. Therefore, the decomposition of ROONO₂ could indeed result in an increase in the RO₂ signal. It should also be pointed out that because of the very short residence time in the chemical ionization inlet, such an increase in the RO₂ concentration would not significantly impact HOM formation.

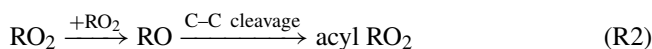
To confirm the reliability of our results, we examined the changes in the signals of RO₂ and closed-shell products as a function of reacted α -pinene in the absence of NO₂ (Sect. S1 and Fig. S7 in the Supplement), and the results are consistent with previous studies (Zhao et al., 2018). In addition, we repeated Exps 15–21 on another nitrate-CIMS, and a similar increase in alkyl RO₂ signals with the addition of NO₂ was observed on that instrument (Fig. S8).

3.2 Formation mechanisms of acyl RO₂ during α -pinene ozonolysis

It has been recently suggested that there are three main pathways that directly lead to the formation of monoterpene-derived acyl RO₂ (Zhao et al., 2022): (i) the autoxidation of RO₂ containing aldehyde groups (Reaction R1), (ii) the cleavage of a C–C bond of RO containing an α -ketone group (Reaction R2), and (iii) the intramolecular H shift of RO containing an aldehyde group (Reaction R3). In addition, the secondary OH oxidation of aldehyde products can also produce acyl RO₂ radicals. However, in the present study, the

secondary OH oxidation is expected to be insignificant due to an excess of α -pinene compared to O₃. Indeed, kinetic model simulations incorporating the secondary OH chemistry show that the contribution of secondary OH oxidation to acyl RO₂ formation is negligible even under high O₃ conditions (see details in Sect. S2 and Fig. S9).

Here, we further investigated the formation mechanisms of acyl RO₂. Figure 4 shows the reaction schemes leading to the formation of example acyl RO₂ radicals. The detailed formation mechanisms of acyl RO₂ measured in this study are shown in Fig. S10. The formation of acyl RO₂, especially those having the small molecular size (C₇–C₉), requires the production and subsequent decomposition (or ring-opening process) of RO radicals. Taking C₈H₁₃O₆-RO₂ as an example (Fig. 4), two steps of RO formation and decomposition following the primary C₁₀H₁₅O₄-RO₂ lead to the ring-opened C₈H₁₃O₄-RO₂ that can undergo rapid aldehydic H shift to form the acyl RO₂.



To verify the formation mechanisms of acyl RO₂, we added NO in some experiments (Exps 33–56) to see how acyl RO₂ respond to the increasing NO concentration. As shown in Fig. 5, the changes of C₇ and C₈ acyl RO₂ show an opposite trend with the increasing NO and NO₂ concentration, except for C₈H₁₃O₈-RO₂. NO can react with RO₂ to form RO radicals and promote the formation of RO₂ that requires the involvement of RO radicals in their formation. In addition to C₈H₁₃O₆-RO₂ discussed above, the formation of C₇H₉O₇-RO₂ and C₈H₁₃O₉-RO₂ needs two and four steps of the RO formation following C₁₀H₁₅O₄-RO₂ (Fig. S10), respectively. Therefore, the increase in RO concentration due to the addition of NO would promote the production of these acyl RO₂. These results prove that the RO radicals indeed play an important role in the acyl RO₂ formation, while for C₈H₁₃O₈-RO₂, its signal decreases substantially with the addition of NO up to 3 ppb, similar to the trend observed with the addition of NO₂. After reaching the minimum at 7 ppb NO, the signal of C₈H₁₃O₈-RO₂ tends to increase with the further increase in NO concentration. Given that C₈H₁₃O₈-RO₂ is likely to directly come from the autoxidation of C₈H₁₃O₆ acyl RO₂ (see Fig. S10), the rapid consumption of C₈H₁₃O₆-RO₂ by NO and NO₂ (formed by O₃ oxidation of NO) may outcompete its autoxidation process, thus leading to a decrease in C₈H₁₃O₈-RO₂ signal. Besides, it can be seen that the increasing extent in C₈H₁₃O₆-RO₂ is also relatively small before the NO concentration reaches 3 ppb (Fig. 5c), indicating that the promotion effect of NO on C₈H₁₃O₆-RO₂ formation is not that strong at this concentration.

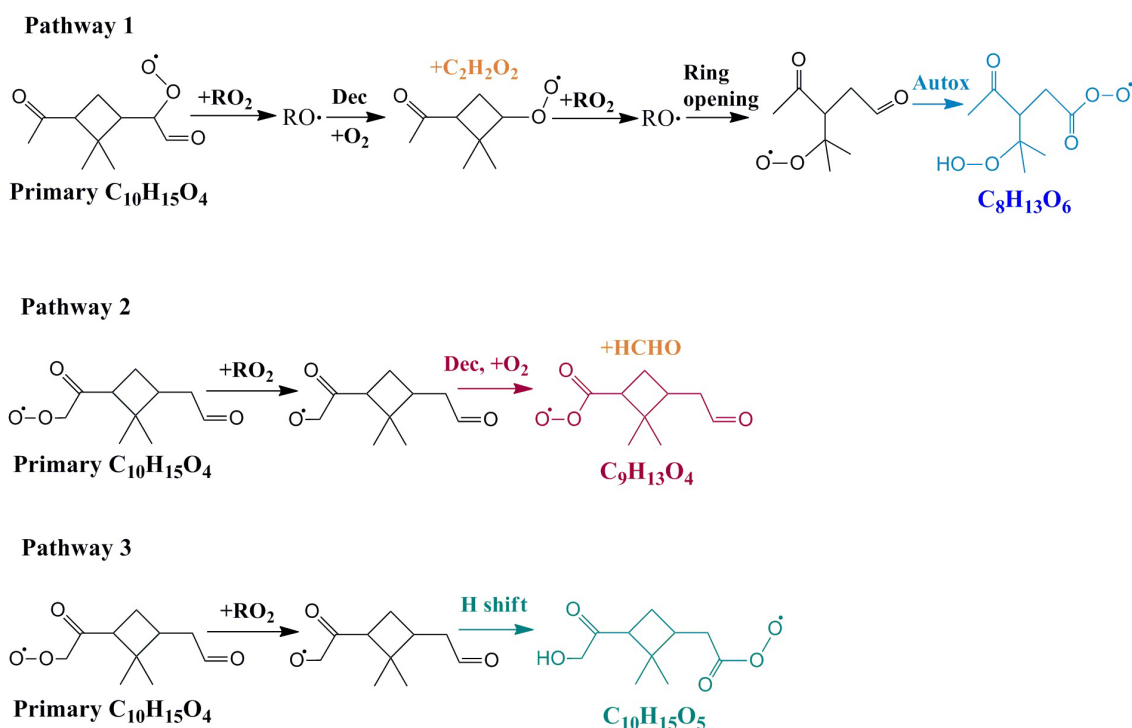


Figure 4. Three different formation pathways of acyl RO_2 during ozonolysis of α -pinene. The acyl RO_2 , $C_9H_{13}O_4$ and $C_{10}H_{15}O_5$, formed via pathways 2 and 3, respectively, were not detected by the nitrate-CIMS in this study due to their relatively low oxygenation level.

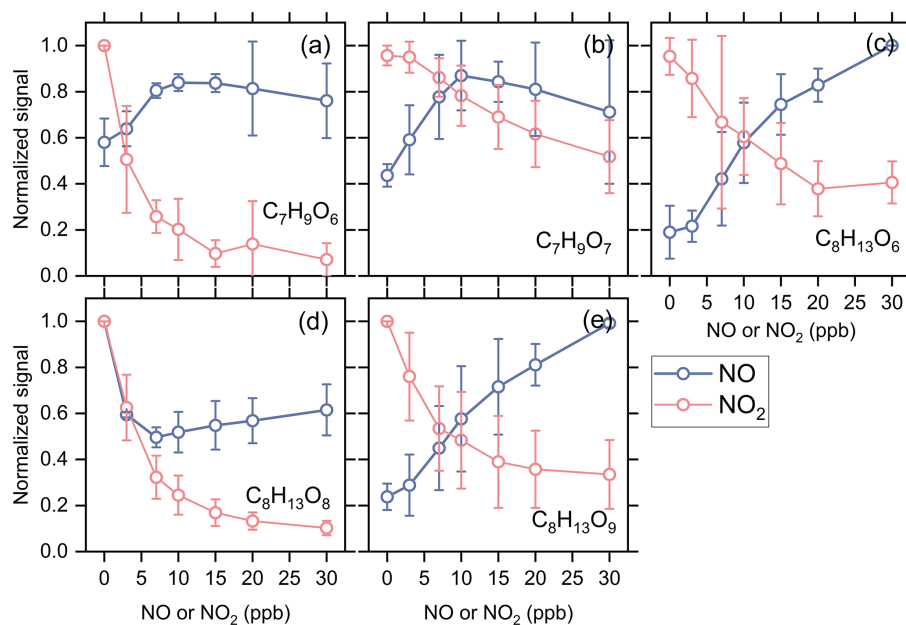


Figure 5. Averaged normalized signal of typical acyl RO_2 as a function of initial NO or NO_2 addition (Exps 1–28 and 33–56).

It is interesting to note that most of the measured highly oxygenated acyl RO_2 are formed by the autoxidation of aldehydic RO_2 , and only the $C_8H_{13}O_9$ - RO_2 is formed by the H shift of the RO radical (Fig. S10). The measured signal of acyl RO_2 from the autoxidation pathway accounts for 96 %

of all highly oxygenated acyl RO_2 signals. Considering that the acyl RO_2 with small molecular size are generally the ring-opened RO_2 , the autoxidation rate constant of their precursor RO_2 is expected to be relatively high (e.g., 1 s^{-1}) (Iyer et al., 2021). Taking a RO_2 cross-reaction rate constant of

$1 \times 10^{-12} \text{ cm}^3 \text{ molec.}^{-1} \text{ s}^{-1}$ (Zhao et al., 2018) and a model-predicted total RO_2 concentration of 1.7 ppb (Exp 8), the simulated contributions of autoxidation and cross-reactions to the total RO_2 reaction are 96.0 % and 4.0 %, respectively. Considering a RO_2 cross-reaction rate constant that is 10 times larger (i.e., $1 \times 10^{-11} \text{ cm}^3 \text{ molec.}^{-1} \text{ s}^{-1}$), the simulated contributions of RO_2 autoxidation and cross-reactions would be 70.4 % and 29.6 %, respectively. These simulations suggest that the autoxidation of aldehydic RO_2 plays a dominant role in the formation of the highly oxygenated acyl RO_2 . Although the acyl RO_2 with low oxygen content were not measured in this study, all acyl RO_2 containing oxygen atoms less than 6 seem to be derived from the cleavage of the C–C bond or H shift of RO containing an α -ketone or aldehyde in the currently known reaction mechanisms (Figs. 4 and S11).

Recently, Shen et al. (2022) found that the hydrogen abstraction by OH radicals during α -pinene oxidation plays an important role in HOM formation. In such mechanisms, the primary RO_2 reacts with NO and forms RO radicals, which could undergo rapid ring-breaking reactions to form a series of ring-opened $\text{C}_{10}\text{H}_{15}\text{O}_x\text{-RO}_2$, which contains aldehyde functionality and can easily autoxidize to C_{10} acyl RO_2 . In the absence of NO, the cross-reactions of RO_2 can also produce RO radicals. However, only a few C_{10} acyl RO_2 were detected in this study, and they contribute less than 1 % of the total C_{10} RO_2 signal. This phenomenon could be due to the fact that the primary RO_2 ($\text{C}_{10}\text{H}_{15}\text{O}_2$) formed by the hydrogen abstraction by OH radical are least oxidized with only 2 oxygen atoms, which are expected to have a relatively low cross-reaction rate constant (Orlando and Tyndall, 2012; Berndt et al., 2018). As a result, the formation of ring-opened $\text{C}_{10}\text{H}_{15}\text{O}_x\text{-RO}_2$ via cross-reactions of the primary $\text{C}_{10}\text{H}_{15}\text{O}_2\text{-RO}_2$ may not be important. As shown in Fig. 6, when the cross-reaction rate constants of $\text{C}_{10}\text{H}_{15}\text{O}_2\text{-RO}_2$ are considered to be $1 \times 10^{-13} \text{ cm}^3 \text{ molec.}^{-1} \text{ s}^{-1}$, the simulated contribution of the H-abstraction pathway to the HOM formation is less than 3 % under both low-reacted (2.4 ppb) and high-reacted (9.6 ppb) α -pinene conditions. It should be noted that the cross-reaction rate constants of the less-oxygenated RO_2 could be even lower (Orlando and Tyndall, 2012); therefore the contribution of this pathway to HOM formation could be ignored when NO is absent.

In the presence of cyclohexane as an OH scavenger (Fig. S12, Exp 32), the measured signals of $\text{C}_{10}\text{H}_{17}\text{O}_x\text{-RO}_2$ formed via the OH addition channel and the corresponding $\text{C}_{10}\text{H}_{18}\text{O}_x$ HOMs decrease by more than 70 %, while the $\text{C}_{10}\text{H}_{15}\text{O}_x\text{-RO}_2$ and its related closed-shell products decrease by less than 15 %, in good agreement with the measurements in previous studies (Zhao et al., 2018). As the $\text{C}_{10}\text{H}_{16}\text{O}_8$ HOM could come from both $\text{C}_{10}\text{H}_{15}\text{O}_x\text{-RO}_2$ and $\text{C}_{10}\text{H}_{17}\text{O}_x\text{-RO}_2$, its reduction is at a medium level. The significantly smaller decrease in the signals of $\text{C}_{10}\text{H}_{15}\text{O}_x\text{-RO}_2$ and its corresponding closed-shell products as compared to those of $\text{C}_{10}\text{H}_{17}\text{O}_x\text{-RO}_2$ and the related closed-shell prod-

ucts further illustrates that the H abstraction by OH has a minor contribution to HOM formation in the absence of NO.

Figure 7 shows the changes in measured signal of $\text{C}_{10}\text{H}_{15}\text{O}_8\text{-RO}_2$ and $\text{C}_{10}\text{H}_{15}\text{O}_{10}\text{-RO}_2$ as a function of initial NO concentration (Exps 33–56). It should be noted that due to the existence of O_3 in our experiments, these two RO_2 could come from both O_3 and OH reactions with α -pinene, and NO could be rapidly oxidized to NO_2 by O_3 . The normalized signals of $\text{C}_{10}\text{H}_{15}\text{O}_8\text{-RO}_2$ and $\text{C}_{10}\text{H}_{15}\text{O}_{10}\text{-RO}_2$ increase firstly under low NO conditions, which is similar to the change of acyl RO_2 as shown in Fig. 5. This increase could be for two reasons: (1) the promoted formation of $\text{C}_{10}\text{H}_{15}\text{O}_8$ and $\text{C}_{10}\text{H}_{15}\text{O}_{10}$ acyl RO_2 from the H-abstraction channel by NO addition and (2) the equilibrium decomposition of ROONO_2 formed by the two alkyl RO_2 from ozonolysis of α -pinene in the chemical ionization inlet (see Sect. 3.1). As mentioned above, the ring-opened $\text{C}_{10}\text{H}_{15}\text{O}_x\text{-RO}_2$ formed from the H-abstraction channel contain aldehyde functionality and can autoxidize rapidly. The FOAM simulations show that the $\text{C}_{10}\text{H}_{15}\text{O}_8$ and $\text{C}_{10}\text{H}_{15}\text{O}_{10}$ acyl RO_2 formed from the H-abstraction channel contribute to 68 % and 56 % of the total $\text{C}_{10}\text{H}_{15}\text{O}_8\text{-RO}_2$ and $\text{C}_{10}\text{H}_{15}\text{O}_{10}\text{-RO}_2$ with the addition of 10 ppb NO, respectively. Therefore, the initial increases of these two RO_2 with increasing NO concentration are likely mainly due to the enhanced formation of $\text{C}_{10}\text{H}_{15}\text{O}_8$ and $\text{C}_{10}\text{H}_{15}\text{O}_{10}$ acyl RO_2 . When the NO concentration increases to a high level, there is more NO and NO_2 in the system, which promotes the consumption of acyl RO_2 . As a result, $\text{C}_{10}\text{H}_{15}\text{O}_8\text{-RO}_2$ exhibits a decreasing trend, and the increasing extend of $\text{C}_{10}\text{H}_{15}\text{O}_{10}\text{-RO}_2$ becomes much smaller.

3.3 Contributions of acyl RO_2 to the formation of gas-phase HOMs

With the addition of NO_2 , the distribution of gas-phase products in the α -pinene ozonolysis changes significantly (see Fig. 1), and the consumption of acyl RO_2 by NO_2 plays an important role. NO_2 influences the formation of HOM monomers mainly in three ways. Firstly, NO_2 could react rapidly with acyl RO_2 and form RC(O)OONO_2 , thus inhibiting the formation of HOMs with the involvement of acyl RO_2 . Secondly, as mentioned above, although ROONO_2 is thermally unstable, their formation–decomposition equilibrium still consumes a small amount of alkyl RO_2 , resulting in a decrease in HOM formation. Thirdly, NO_2 can consume a part of HO_2 radicals (Fig. S13), thus inhibiting the $\text{RO}_2 + \text{HO}_2$ reaction pathway.

Figure 8 shows the normalized signal of $\text{C}_7\text{–C}_{10}$ HOM monomers as a function of initial NO_2 concentration. The signals of C_7 , C_8 , and some of C_9 HOMs decrease significantly with increasing NO_2 concentration due to the relatively large contribution of acyl RO_2 to the total $\text{C}_7\text{–C}_9$ RO_2 . The C_7 HOMs decrease by more than 50 % when the NO_2 concentration reaches 30 ppb, while C_8 HOMs decrease by

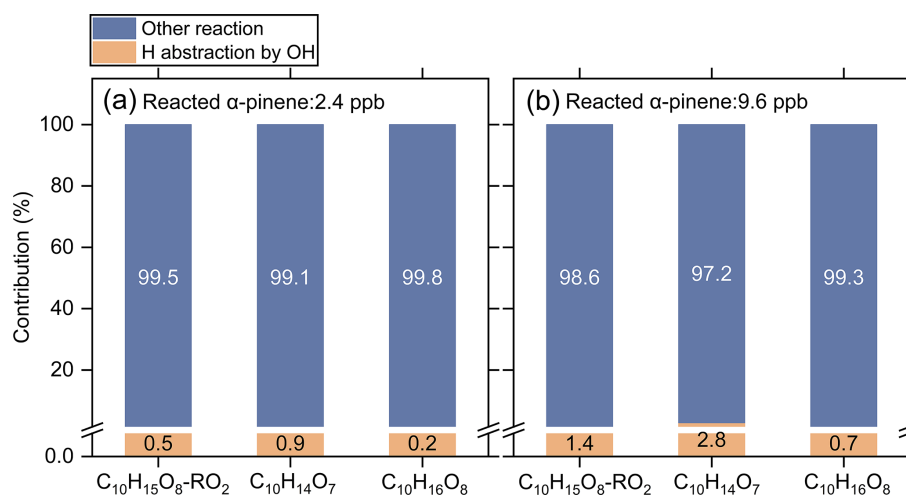


Figure 6. Contributions of the H-abstraction pathway by OH radicals (yellow) and OH addition and ozonolysis pathways (blue) to the formation of typical HOMs under low-reacted (a) and high-reacted (b) α -pinene conditions simulated by the kinetic model. The cross-reaction rate constant was set to $1 \times 10^{-13} \text{ cm}^3 \text{ molec.}^{-1} \text{ s}^{-1}$ for the primary $C_{10}H_{15}O_2-RO_2$ and $1 \times 10^{-12} \text{ cm}^3 \text{ molec.}^{-1} \text{ s}^{-1}$ for the more oxygenated RO_2 .

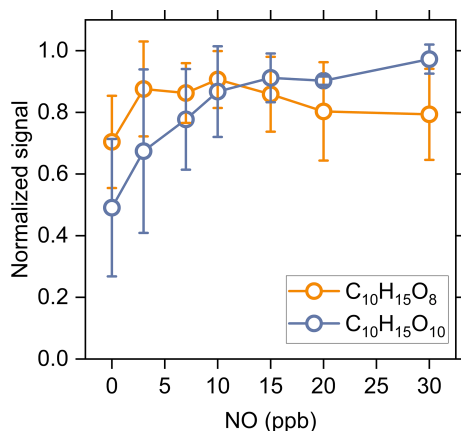


Figure 7. Averaged normalized signal of the measured $C_{10}H_{15}O_8-$ and $C_{10}H_{15}O_{10}-RO_2$ as a function of the added NO concentration (Exps 33–56).

more than 70 %, and some of them even decrease by 90 %. The C_9 HOMs decrease by 30 %–60 %, and the species with relatively large decrease are mostly acyl RO_2 -related HOMs. For C_{10} HOMs, although there is also an obvious decrease in their formation with the addition of NO_2 , most of them have a smaller decreasing extent compared to the C_7 – C_9 HOMs due to the low contribution of acyl RO_2 to the C_{10} RO_2 . It is worth noting that a few C_{10} HOMs increase initially with the addition of NO_2 up to 10 ppb, suggesting that there might be some processes that promote the formation of their precursor RO_2 radicals and thus offset the inhibiting effect of NO_2 .

As mentioned above, the addition of NO_2 has the most significant influence on the formation of small HOM monomers. Combined with the large contribution (67 %–94 %) of acyl

RO_2 to the total C_7 and C_8 RO_2 (Fig. 3), it can be considered that the reduction in the formation of C_7 and C_8 HOM monomers with NO_2 addition is overwhelmingly due to the consumption of acyl RO_2 by NO_2 . As a result, acyl RO_2 were found to have a contribution of 50 %–90 % to C_7 and C_8 HOM monomer formation during α -pinene ozonolysis. Since acyl RO_2 also have a considerable contribution (32 %) to the total C_9 RO_2 , an upper limit (30 %–60 %) of their contribution to C_9 HOMs could be derived with the assumption that the decrease of C_9 HOMs with the addition of NO_2 is also mainly due to the consumption of C_9 -acyl RO_2 by NO_2 . By contrast, acyl RO_2 account for a very small fraction (0.4 %) of the total C_{10} RO_2 , and their contribution to C_{10} HOMs cannot be quantified based solely on the experimental measurements given that the equilibrium reaction between alkyl RO_2 and NO_2 can also affect the formation of HOMs. Therefore, we used F0AM to simulate the contribution of acyl RO_2 to C_{10} HOM formation according to the acyl RO_2 measured in this study. It should be noted that the HOMs from the acyl RO_2 and its subsequent RO_2 (formed from acyl RO_2 reactions) are all considered to be acyl- RO_2 -related HOMs in the model.

As mentioned above, the formation of ring-opened $C_{10}H_{15}O_4-RO_2$ reported by Iyer et al. (2021) is included in the model, and its autoxidation produces a ring-opened acyl $C_{10}H_{15}O_8-RO_2$. When we consider the upper limit of the yield of ring-opened $C_{10}H_{15}O_4-RO_2$ (89 %) in the model and assume that the other primary RO_2 with the cyclobutyl ring autoxidize at a very slow rate (0.01 s^{-1}), the simulated acyl $C_{10}H_{15}O_8-RO_2$ would contribute to ~ 80 % of the total C_{10} RO_2 . However, we could not see a large decrease in the measured signal of $C_{10}H_{15}O_8-RO_2$ and its related HOM monomers with the addition of NO_2 . Similarly, a recent

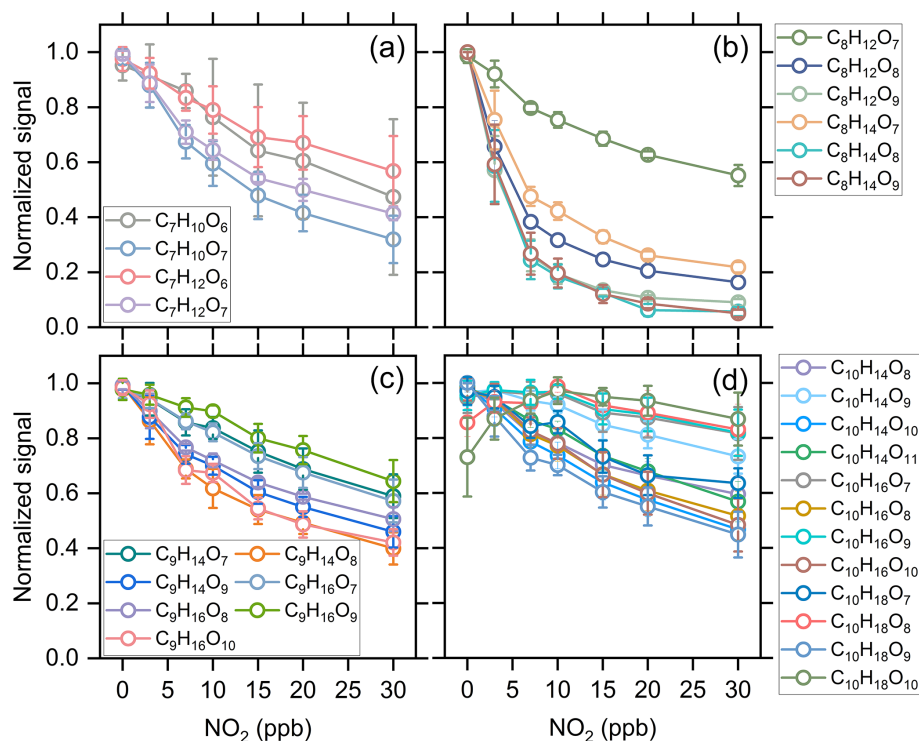


Figure 8. Averaged normalized signal of the measured C₇–C₁₀ HOMs as a function of the added NO₂ concentration (Exps 1–28).

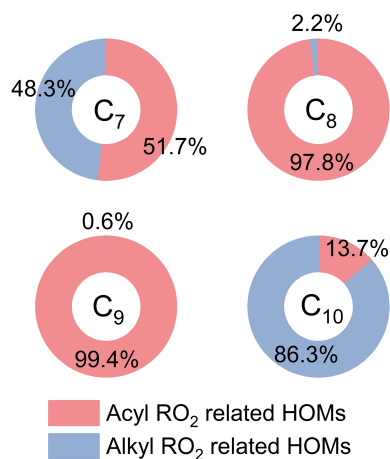


Figure 9. Simulated average contribution of acyl and alkyl RO₂ to C₇–C₁₀ HOM formation from ozonolysis of α -pinene under typical experimental conditions (Exps 1, 8, 15, and 22).

study by Zhao et al. (2022) found that the C₁₀H₁₅O₈-related monomers and dimers in α -pinene SOA did not significantly decrease with NO₂ addition. There might be three reasons for the discrepancy between the simulations and measurements. Firstly, the yield of the ring-opened C₁₀H₁₅O₄-RO₂ might be significantly smaller than 89% (Zhao et al., 2021; Meder et al., 2023). Secondly, the autoxidation rate of other primary C₁₀H₁₅O₄-RO₂ with the cyclobutyl ring could be

significantly larger than 0.01 s⁻¹. Thirdly, the ring-opened C₁₀H₁₅O₈-RO₂, a highly functionalized acyl RO₂ radical with an –OOH group, may be able to undergo very fast intramolecular H-scrambling reactions to form a peroxy acid as suggested by Knap and Jørgensen (2017), which would compete with the NO₂ reaction and result in a lower reduction in its signal upon NO₂ addition (see details in Sect. S3).

To examine the contributions of acyl RO₂ to C₁₀ HOM production, we updated the branching ratios and autoxidation rates of the primary RO₂ during α -pinene ozonolysis in the model according to the recent studies (Kurten et al., 2015; Claffin et al., 2018; Zhao et al., 2021; Berndt, 2022) (Table S3) and used a lower limit (30%) of the ring-opened C₁₀H₁₅O₄-RO₂ yield reported by Iyer et al. (2021). As displayed in Fig. 9, the simulated acyl RO₂-related HOMs contribute to 14% of the total C₁₀ HOMs, which is slightly smaller than the measured decrease in C₁₀ HOMs with the addition of NO₂. This discrepancy could be for two reasons. Firstly, the decrease in HOMs can partly result from the consumption of alkyl RO₂ and HO₂ radicals by the addition of NO₂. Secondly, as mentioned above, there might be other C₁₀ acyl RO₂ that were not observed in this study due to the decomposition of the ROONO₂ from the alkyl RO₂ with the same formulas. The contributions of acyl RO₂ to the formation of C₇–C₉ HOMs were also simulated (Fig. 9). For C₇ and C₈ HOMs, the model predicts a contribution of 52%–98% from acyl RO₂, which is consistent with the measurements (50%–90%). However, the simulated contribution of

acyl RO₂ to C₉ HOMs is over 99 %, which is not consistent with the measurements (Fig. 8c). Recent studies indicated that the CI radicals from α -pinene ozonolysis did not form the alkyl C₉H₁₅O₃-RO₂ (C96O2 in default MCM v3.3.1) (Kurten et al., 2015; Zhao et al., 2021; Berndt, 2022). As a result, this primary C₉ alkyl RO₂ was not considered in the model, and most of C₉ RO₂ considered are acyl RO₂ or from acyl RO₂ reactions. In view of the significantly lower measured (less than 30 %–60 %) than simulated (over 99 %) contribution of acyl RO₂ to C₉ HOMs, we speculate that a small part of CI radicals might be able to form the C₉H₁₅O₃-RO₂, which could further react to form highly oxygenated alkyl C₉ RO₂.

A sensitivity analysis of the alkyl C₉H₁₅O₃-RO₂ yield was conducted to see its influence on the contribution of acyl RO₂ to the total C₉ HOMs. The model simulations show that when the yield of this C₉ RO₂ from one of the CIs ranges between 0.5 % and 2 %, the contribution of acyl RO₂ to the total C₉ HOMs ranges from 27.5 % to 59.8 % (Fig. S15), which is almost consistent with the measurements. This result indicates that a small part of CIs could generate the C₉ alkyl RO₂. We note that the small production of C₉H₁₅O₃-RO₂ from CIs has no significant influence on the yield of C₁₀H₁₅O₄-RO₂ and the subsequent acyl RO₂. As shown in Fig. S16, as the C₉H₁₅O₃-RO₂ yield increases from 0 % to 3 %, the simulated concentrations of C₁₀H₁₅O₄-RO₂ exhibit negligible to small (5 %) changes. As the C₉H₁₅O₃-RO₂ is considered to only produce highly oxygenated alkyl RO₂ in the model, it results in a decrease in the contribution of acyl RO₂ to the total C₉ HOMs. However, the contributions of acyl RO₂ to total C₇, C₈, and C₁₀ HOMs are almost unchanged.

The cross-reaction rate constant of acyl RO₂ is generally larger than that of alkyl RO₂ (Atkinson et al., 2007; Orlando and Tyndall, 2012), and the fast cross-reaction may lead to an important contribution to the HOM dimer production. The responses of dimer formation to increasing concentration of initial NO₂ during α -pinene ozonolysis are given in Fig. 10. The C₁₄–C₁₈ dimers decrease by up to 50 %–95 % with the increase in NO₂ concentration up to 30 ppb (Fig. 10a–e). The rapid cross-reaction rate of acyl RO₂, as well as their dominant contribution to the small RO₂ species, makes acyl RO₂ an important contributor to the formation of these dimers. The consumption of acyl RO₂ by NO₂ greatly inhibits the bimolecular reactions involving acyl RO₂, resulting in a rapid decrease in the signal of the corresponding dimers. Considering the predominance of acyl RO₂ in small RO₂ and their high reaction rate with NO₂ compared to the alkyl RO₂, it can be concluded that the cross-reactions involving acyl RO₂ contribute to roughly 50 %–95 % of the C₁₄–C₁₈ dimer formation.

For C₁₉ dimers, due to the relatively smaller contribution of acyl RO₂ to C₉ and C₁₀ RO₂, their signal decreases only by 10 %–40 %, and this reduction has contributions from both acyl and alkyl RO₂. For C₂₀ dimers, their signal changes with the addition of NO₂ can be discussed ac-

ording to the number of hydrogen atoms in the molecules. Firstly, the signals of C₂₀H₃₀O₇ and C₂₀H₃₀O₉ decrease by 40 %–60 % with the addition of 30 ppb NO₂, indicating a significant contribution of acyl RO₂ such as C₁₀H₁₅O₅-RO₂ (acyl RO₂ in default MCM v3.3.1) and C₁₀H₁₅O₇-RO₂ in their formation, while other C₂₀H₃₀O_x dimers decrease by ~ 30 %. The C₂₀H₃₂O_x dimer series also exhibits a small reduction (less than 20 %) with the addition of NO₂. However, the C₂₀H₃₄O_x series shows an unexpected increase with the addition of NO₂ up to 10 ppb and almost remains unchanged with the further increase in NO₂ concentration. Given that the cross-reaction rate constant of acyl RO₂ can be orders of magnitude higher than that of counterpart alkyl RO₂ (Atkinson et al., 2007; Orlando and Tyndall, 2012), the rapid consumption of acyl RO₂ by NO₂ would preserve the alkyl RO₂ that tend to react with acyl RO₂ at a fast rate in the absence of NO₂, which to some extent would elevate the concentration of alkyl RO₂ in the system and thus promote the less competitive alkyl RO₂ + alkyl RO₂ reactions to form C₂₀H₃₄O_x dimers. The slight increase in some C₁₀H₁₈O_x HOMs with the addition of NO₂ up to 10 ppb could also be for this reason.

According to the noticeable increasing trend in C₂₀H₃₄O_x as compared to other C₂₀ dimers, we speculate that acyl RO₂ react faster with C₁₀H₁₇O_x alkyl RO₂ than with C₁₀H₁₅O_x alkyl RO₂. Therefore, when the acyl RO₂ are depleted, the preservation of C₁₀H₁₇O_x-RO₂ is more significant, and the promotion of their cross-reactions to form C₂₀H₃₄O_x is more evident. It is also possible that the reaction of NO₂ with C₁₀H₁₇O_x alkyl RO₂ is less efficient compared to the reaction with C₁₀H₁₅O_x alkyl RO₂, so more C₁₀H₁₇O_x than C₁₀H₁₅O_x is available for dimer formation in the presence of NO₂.

To further prove the above two speculations, we performed sensitivity analyses for the reaction rates of C₁₀H₁₇O_x-RO₂ using FOAM. Figure 11a shows the changes in C₂₀H₃₄O_x dimers with NO₂ addition at different C₁₀H₁₇O_x-RO₂ + NO₂ reaction rates under the conditions of Exps 8–14. As the reaction rate varies from 1×10^{-13} to 1×10^{-12} cm³ molec.⁻¹ s⁻¹, the increasing trend of C₂₀H₃₄O_x dimers versus the added NO₂ concentration is weakened, and the simulation is more deviated from the measurements. When the reaction rate increases to 7.5×10^{-12} cm³ molec.⁻¹ s⁻¹, the C₂₀H₃₄O_x dimers decrease significantly with increasing NO₂, which is in striking contrast to the measurements. Figure 11b presents the sensitivity analysis results for the cross-reaction rate constants of acyl RO₂ + C₁₀H₁₇O_x-RO₂. As this rate constant varies from 1×10^{-12} to 1×10^{-10} cm³ molec.⁻¹ s⁻¹, the increasing trend of C₂₀H₃₄O_x versus the NO₂ concentration is more pronounced and more consistent with the measurements. These sensitivity analyses support our speculation that the C₁₀H₁₇O_x alkyl RO₂ may be different from other alkyl RO₂ radicals in terms of the reaction efficiency with NO₂ and acyl RO₂ species, which leads to different responses of C₂₀H₃₄O_x

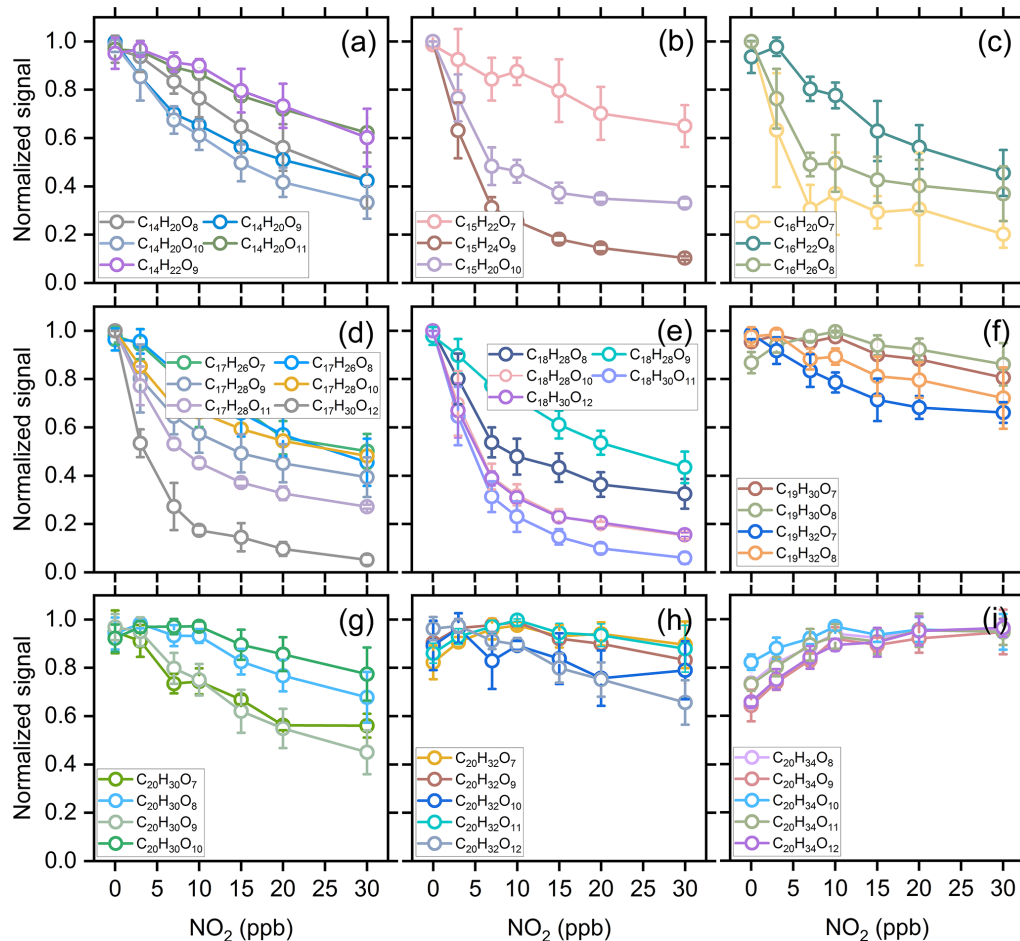


Figure 10. Averaged normalized signal of the measured C_{14} – C_{20} dimers as a function of the added NO_2 concentration (Exps 1–28).

dimers to NO_2 addition compared to other C_{20} dimers. These results also suggest that the presence of acyl RO_2 could affect the fate and contribution of alkyl RO_2 to HOM formation in atmospheric oxidation systems given the different reactivity of acyl RO_2 from alkyl RO_2 .

4 Conclusions

In this study, the molecular identities, formation mechanisms, and contributions of acyl RO_2 to the formation of HOMs during ozonolysis of α -pinene are investigated using a combination of flow reactor experiments and detailed kinetic model simulations. Based on the marked decrease in RO_2 signal as a function of initial NO_2 concentration, a total of 10 highly oxygenated acyl RO_2 are identified during α -pinene ozonolysis. The acyl RO_2 contribute to 67 %, 94 %, and 32 % of C_7 , C_8 , and C_9 highly oxygenated RO_2 but only 0.4 % of C_{10} highly oxygenated RO_2 , respectively, when NO is absent. Three main pathways are identified for the formation of monoterpene-derived acyl RO_2 : (i) the autoxidation of RO_2 containing aldehyde groups, (ii) the cleavage of a C–C bond

of RO containing an α -ketone group, and (iii) the intramolecular H shift of RO containing an aldehyde group. The autoxidation of aldehydic RO_2 formed involving multiple RO decomposition or ring-opening steps plays a dominant role in the formation of the highly oxygenated acyl RO_2 radicals (oxygen atom number ≥ 6), while the less-oxygenated acyl RO_2 (oxygen atom number < 6) are mainly derived from the other two pathways.

The acyl- RO_2 -involved reactions explain 50 %–90 % of C_7 and C_8 HOM monomers and 14 % of C_{10} HOMs, respectively. For C_9 HOMs, this contribution can be up to 30 %–60 %. For the HOM dimers, acyl- RO_2 -involved reactions contribute 50 %–95 % to the formation of C_{14} – C_{18} dimers. Owing to the higher cross-reaction rate constant of acyl RO_2 compared to alkyl RO_2 , the acyl RO_2 + alkyl RO_2 reaction would outcompete the alkyl RO_2 + alkyl RO_2 reaction. Therefore, the rapid consumption of acyl RO_2 by NO_2 in the experiments (as well as in polluted atmospheres) would make the alkyl RO_2 that are supposed to react with acyl RO_2 retained, which to some extent elevates the concentration of alkyl RO_2 in the system and thus promotes the reaction of

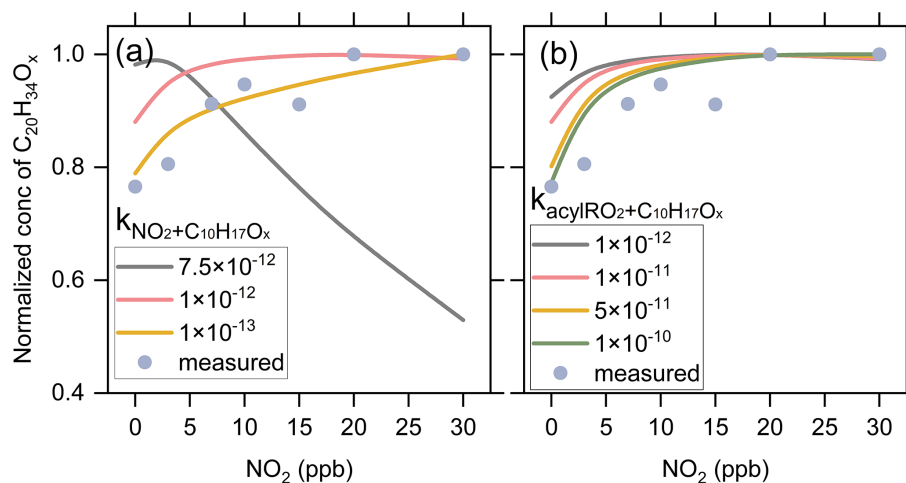


Figure 11. Sensitivity of $C_{20}H_{34}O_x$ dimer production to (a) the reaction rates of NO_2 with $C_{10}H_{17}O_x$ - RO_2 and (b) the cross-reaction rate of acyl RO_2 with $C_{10}H_{17}O_x$ - RO_2 considering a $C_{10}H_{17}O_x$ - $RO_2 + NO_2$ reaction rate of $1 \times 10^{-12} \text{ cm}^3 \text{ molec.}^{-1} \text{ s}^{-1}$.

alkyl $RO_2 +$ alkyl RO_2 to form dimers such as $C_{20}H_{34}O_x$. The contribution of H abstraction of α -pinene by OH radical to the formation of acyl RO_2 and HOMs is found to be negligible in the absence of NO. This is because the primary $C_{10}H_{15}O_2$ - RO_2 radicals formed in such pathways are least-oxidized and thus have relatively low cross-reaction efficiency to produce RO radicals, which are the key intermediates for the formation of acyl RO_2 and HOMs in that channel. However, in the presence of NO, the formation of highly oxygenated acyl RO_2 via the H-abstraction pathway is demonstrated, consistent with previous studies (Shen et al., 2022).

In this study, acyl RO_2 species are identified according to a dramatic decrease in their signals with the addition of NO_2 . It should be noted that the presence of NO_2 could also inhibit the formation of alkyl RO_2 species involving acyl RO_2 reactions. If there are any contributions of alkyl RO_2 to acyl RO_2 identified in this study, the influence of such alkyl RO_2 species on HOM formation would reflect an indirect effect of acyl RO_2 . However, given that the formation of most of the acyl RO_2 identified in this study can be reasonably explained by the proposed mechanisms and verified by their responses to the addition of NO, the acyl RO_2 identified here are expected to have no significant contributions from alkyl RO_2 . Currently, the reaction kinetics of monoterpene-derived acyl RO_2 are still poorly understood. Considering the important contribution of acyl RO_2 to HOM formation, further kinetic studies are needed to get more specific rate constants for their autoxidation and cross-reactions, thereby deepening our understanding of the role of acyl RO_2 in HOM and SOA formation under atmospheric conditions.

Data availability. The data presented in this work are available upon request from the corresponding author.

Supplement. The supplement related to this article is available online at: <https://doi.org/10.5194/acp-23-12691-2023-supplement>.

Author contributions. YZ and HZ designed the study, and HZ, DH, and JZ performed the experiments. YZ and HZ analyzed the data, conducted model simulations, and wrote the paper. All other authors contributed to the discussion and writing.

Competing interests. The contact author has declared that none of the authors has any competing interests.

Disclaimer. Publisher's note: Copernicus Publications remains neutral with regard to jurisdictional claims made in the text, published maps, institutional affiliations, or any other geographical representation in this paper. While Copernicus Publications makes every effort to include appropriate place names, the final responsibility lies with the authors.

Acknowledgements. Yue Zhao acknowledges the Program for Professor of Special Appointment (Eastern Scholar) at Shanghai Institutions of Higher Learning.

Financial support. This research has been supported by the National Natural Science Foundation of China (grant nos. 22022607, 21806104, and 42005090) and the Program for Professor of Special Appointment (Eastern Scholar) at Shanghai Institutions of Higher Learning.

Review statement. This paper was edited by John Liggio and reviewed by two anonymous referees.

References

- Atkinson, R., Hasegawa, D., and Aschmann, S. M.: Rate constants for the gas-phase reactions of O_3 with a series of monoterpenes and related compounds at 296 ± 2 K, *Int. J. Chem. Kinet.*, 22, 871–887, <https://doi.org/10.1002/kin.550220807>, 1990.
- Atkinson, R., Baulch, D. L., Cox, R. A., Crowley, J. N., Hampson, R. F., Hynes, R. G., Jenkin, M. E., Rossi, M. J., and Troe, J.: Evaluated kinetic and photochemical data for atmospheric chemistry: Volume III – gas phase reactions of inorganic halogens, *Atmos. Chem. Phys.*, 7, 981–1191, <https://doi.org/10.5194/acp-7-981-2007>, 2007.
- Bell, D. M., Wu, C., Bertrand, A., Graham, E., Schoonbaert, J., Giannoukos, S., Baltensperger, U., Prevot, A. S. H., Riipinen, I., El Haddad, I., and Mohr, C.: Particle-phase processing of α -pinene NO_3 secondary organic aerosol in the dark, *Atmos. Chem. Phys.*, 22, 13167–13182, <https://doi.org/10.5194/acp-22-13167-2022>, 2022.
- Berndt, T.: Peroxy radical processes and product formation in the OH radical-initiated oxidation of α -pinene for near-atmospheric conditions, *J. Phys. Chem. A*, 125, 9151–9160, <https://doi.org/10.1021/acs.jpca.1c05576>, 2021.
- Berndt, T.: Peroxy radical and product formation in the gas-phase ozonolysis of α -pinene under near-atmospheric conditions: occurrence of an additional series of peroxy radicals $O, O-C_{10}H_{15}O(O_2)_yO_2$ with $y = 1-3$, *J. Phys. Chem. A*, 126, 6526–6537, <https://doi.org/10.1021/acs.jpca.2c05094>, 2022.
- Berndt, T., Richters, S., Jokinen, T., Hyttinen, N., Kurtén, T., Otkjær, R. V., Kjaergaard, H. G., Stratmann, F., Herrmann, H., and Sipilä, M.: Hydroxyl radical-induced formation of highly oxidized organic compounds, *Nat. Commun.*, 7, 1–8, <https://doi.org/10.1038/ncomms13677>, 2016.
- Berndt, T., Mentler, B., Scholz, W., Fischer, L., Herrmann, H., Kulmala, M., and Hansel, A.: Accretion product formation from ozonolysis and OH radical reaction of α -pinene: mechanistic insight and the influence of isoprene and ethylene, *Environ. Sci. Technol.*, 52, 11069–11077, <https://doi.org/10.1021/acs.est.8b02210>, 2018.
- Bianchi, F., Kurteïn, T., Riva, M., Mohr, C., Rissanen, M. P., Roldin, P., Berndt, T., Crouse, J. D., Wennberg, P. O., and Mentel, T. F.: Highly oxygenated organic molecules (HOM) from gas-phase autoxidation involving peroxy radicals: A key contributor to atmospheric aerosol, *Chem. Rev.*, 119, 3472–3509, 2019.
- Calvert, J. G., Derwent, R. G., Orlando, J. J., Wallington, T. J., and Tyndall, G. S.: Mechanisms of atmospheric oxidation of the alkanes, Oxford University Press, Oxford, 992 pp., ISBN: 978-0195365818, 2008.
- Clafin, M. S., Krechmer, J. E., Hu, W., Jimenez, J. L., and Ziemann, P. J.: Functional group composition of secondary organic aerosol formed from ozonolysis of α -pinene under high VOC and autoxidation conditions, *ACS Earth Space Chem.*, 2, 1196–1210, <https://doi.org/10.1021/acsearthspacechem.8b00117>, 2018.
- Ehn, M., Thornton, J. A., Kleist, E., Sipilä, M., Junninen, H., Pullinen, I., Springer, M., Rubach, F., Tillmann, R., and Lee, B.: A large source of low-volatility secondary organic aerosol, *Nature*, 506, 476–479, <https://doi.org/10.1038/nature13032>, 2014.
- Fry, J. L., Kiendler-Scharr, A., Rollins, A. W., Wooldrige, P. J., Brown, S. S., Fuchs, H., Dubé, W., Mensah, A., dal Maso, M., Tillmann, R., Dorn, H.-P., Brauers, T., and Cohen, R. C.: Organic nitrate and secondary organic aerosol yield from NO_3 oxidation of β -pinene evaluated using a gas-phase kinetics/aerosol partitioning model, *Atmos. Chem. Phys.*, 9, 1431–1449, <https://doi.org/10.5194/acp-9-1431-2009>, 2009.
- Fry, J. L., Draper, D. C., Barsanti, K. C., Smith, J. N., Ortega, J., Winkler, P. M., Lawler, M. J., Brown, S. S., Edwards, P. M., and Cohen, R. C.: Secondary organic aerosol formation and organic nitrate yield from NO_3 oxidation of biogenic hydrocarbons, *Environ. Sci. Technol.*, 48, 11944–11953, <https://doi.org/10.1021/es502204x>, 2014.
- Guenther, A. B., Jiang, X., Heald, C. L., Sakulyanontvittaya, T., Duhl, T., Emmons, L. K., and Wang, X.: The Model of Emissions of Gases and Aerosols from Nature version 2.1 (MEGAN2.1): an extended and updated framework for modeling biogenic emissions, *Geosci. Model Dev.*, 5, 1471–1492, <https://doi.org/10.5194/gmd-5-1471-2012>, 2012.
- Iyer, S., Rissanen, M. P., Valiev, R., Barua, S., Krechmer, J. E., Thornton, J., Ehn, M., and Kurten, T.: Molecular mechanism for rapid autoxidation in alpha-pinene ozonolysis, *Nat. Commun.*, 12, 878, <https://doi.org/10.1038/s41467-021-21172-w>, 2021.
- Jenkin, M. E., Young, J. C., and Rickard, A. R.: The MCM v3.3.1 degradation scheme for isoprene, *Atmos. Chem. Phys.*, 15, 11433–11459, <https://doi.org/10.5194/acp-15-11433-2015>, 2015.
- Jokinen, T., Sipilä, M., Richters, S., Kerminen, V. M., Paasonen, P., Stratmann, F., Worsnop, D., Kulmala, M., Ehn, M., and Herrmann, H.: Rapid autoxidation forms highly oxidized RO_2 radicals in the atmosphere, *Angew. Chem. Int. Edit.*, 53, 14596–14600, <https://doi.org/10.1002/anie.201408566>, 2014.
- Junninen, H., Ehn, M., Petäjä, T., Luosujärvi, L., Kotiaho, T., Kostianen, R., Rohner, U., Gonin, M., Fuhrer, K., Kulmala, M., and Worsnop, D. R.: A high-resolution mass spectrometer to measure atmospheric ion composition, *Atmos. Meas. Tech.*, 3, 1039–1053, <https://doi.org/10.5194/amt-3-1039-2010>, 2010.
- Kirchner, F., Thuener, L., Barnes, I., Becker, K., Donner, B., and Zabel, F.: Thermal lifetimes of peroxy nitrates occurring in the atmospheric degradation of oxygenated fuel additives, *Environ. Sci. Technol.*, 31, 1801–1804, <https://doi.org/10.1021/es9609415>, 1997.
- Knap, H. C. and Jørgensen, S.: Rapid Hydrogen Shift Reactions in Acyl Peroxy Radicals, *J. Phys. Chem. A*, 121, 1470–1479, <https://doi.org/10.1021/acs.jpca.6b12787>, 2017.
- Knopf, D. A., Pöschl, U., and Shiraiwa, M.: Radial diffusion and penetration of gas molecules and aerosol particles through laminar flow reactors, denuders, and sampling tubes, *Anal. Chem.*, 87, 3746–3754, <https://doi.org/10.1021/ac5042395>, 2015.
- Kristensen, K., Watne, Å. K., Hammes, J., Lutz, A., Petäjä, T., Hallquist, M., Bilde, M., and Glasius, M.: High-molecular weight dimer esters are major products in aerosols from α -pinene ozonolysis and the boreal forest, *Environ. Sci. Tech. Lett.*, 3, 280–285, 2016.
- Kurten, T., Rissanen, M. P., Mackeprang, K., Thornton, J. A., Hyttinen, N., Jørgensen, S., Ehn, M., and Kjaergaard, H. G.: Computational study of hydrogen shifts and ring-opening mechanisms in alpha-pinene ozonolysis products, *J. Phys. Chem. A*, 119, 11366–11375, <https://doi.org/10.1021/acs.jpca.5b08948>, 2015.
- Li, X., Chee, S., Hao, J., Abbatt, J. P. D., Jiang, J., and Smith, J. N.: Relative humidity effect on the formation of highly oxidized molecules and new particles during monoterpene oxidation, *At-*

- mos. Chem. Phys., 19, 1555–1570, <https://doi.org/10.5194/acp-19-1555-2019>, 2019.
- Lin, C., Huang, R.-J., Duan, J., Zhong, H., and Xu, W.: Primary and secondary organic nitrate in northwest China: a case study, *Environ. Sci. Tech. Let.*, 8, 947–953, <https://doi.org/10.1021/acs.estlett.1c00692>, 2021.
- Meder, M., Peräkylä, O., Varelas, J. G., Luo, J., Cai, R., Zhang, Y., Kurtén, T., Riva, M., Rissanen, M., Geiger, F. M., Thomson, R. J., and Ehn, M.: Selective deuteration as a tool for resolving autoxidation mechanisms in α -pinene ozonolysis, *Atmos. Chem. Phys.*, 23, 4373–4390, <https://doi.org/10.5194/acp-23-4373-2023>, 2023.
- Mentel, T. F., Springer, M., Ehn, M., Kleist, E., Pullinen, I., Kurtén, T., Rissanen, M., Wahner, A., and Wildt, J.: Formation of highly oxidized multifunctional compounds: autoxidation of peroxy radicals formed in the ozonolysis of alkenes – deduced from structure–product relationships, *Atmos. Chem. Phys.*, 15, 6745–6765, <https://doi.org/10.5194/acp-15-6745-2015>, 2015.
- Molteni, U., Simon, M., Heinritzi, M., Hoyle, C. R., Bernhammer, A.-K., Bianchi, F., Breitenlechner, M., Brilke, S., Dias, A., Duplissy, J., Frege, C., Gordon, H., Heyn, C., Jokinen, T., Kürten, A., Lehtipalo, K., Makhmutov, V., Petäjä, T., Pieber, S. M., Praplan, A. P., Schobesberger, S., Steiner, G., Stozhkov, Y., Tomé, A., Tröstl, J., Wagner, A. C., Wagner, R., Williamson, C., Yan, C., Baltensperger, U., Curtius, J., Donahue, N. M., Hansel, A., Kirkby, J., Kulmala, M., Worsnop, D. R., and Dommen, J.: Formation of highly oxygenated organic molecules from α -pinene ozonolysis: chemical characteristics, mechanism, and kinetic model development, *ACS Earth Space Chem.*, 3, 873–883, <https://doi.org/10.1021/acsearthspacechem.9b00035>, 2019.
- Nozière, B., Kalberer, M., Claeys, M., Allan, J., D’Anna, B., Decesari, S., Finessi, E., Glasius, M., Grgic, I., and Hamilton, J. F.: The molecular identification of organic compounds in the atmosphere: state of the art and challenges, *Chem. Rev.*, 115, 3919–3983, 2015.
- Orlando, J. J. and Tyndall, G. S.: Laboratory studies of organic peroxy radical chemistry: an overview with emphasis on recent issues of atmospheric significance, *Chem. Soc. Rev.*, 41, 6294–6317, <https://doi.org/10.1039/C2CS35166H>, 2012.
- Otkjær, R. V., Jakobsen, H. H., Tram, C. M., and Kjaergaard, H. G.: Calculated hydrogen shift rate constants in substituted alkyl peroxy radicals, *J. Phys. Chem. A*, 122, 8665–8673, <https://doi.org/10.1021/acs.jpca.8b06223>, 2018.
- Pye, H. O. T., Chan, A. W. H., Barkley, M. P., and Seinfeld, J. H.: Global modeling of organic aerosol: the importance of reactive nitrogen (NO_x and NO_3), *Atmos. Chem. Phys.*, 10, 11261–11276, <https://doi.org/10.5194/acp-10-11261-2010>, 2010.
- Atkinson, R., Aschmann, S. M., and Pitts Jr., J. N.: Rate constants for the gas-phase reactions of the OH radical with a series of monoterpenes at 294 ± 1 K, *Int. J. Chem. Kinet.*, 18, 287–299, <https://doi.org/10.1002/kin.550180303>, 1986.
- Shen, H., Vereecken, L., Kang, S., Pullinen, I., Fuchs, H., Zhao, D., and Mentel, T. F.: Unexpected significance of a minor reaction pathway in daytime formation of biogenic highly oxygenated organic compounds, *Sci. Adv.*, 8, eabp8702, <https://doi.org/10.1126/sciadv.abp8702>, 2022.
- Sindelarova, K., Granier, C., Bouarar, I., Guenther, A., Tilmes, S., Stavrou, T., Müller, J.-F., Kuhn, U., Stefani, P., and Knorr, W.: Global data set of biogenic VOC emissions calculated by the MEGAN model over the last 30 years, *Atmos. Chem. Phys.*, 14, 9317–9341, <https://doi.org/10.5194/acp-14-9317-2014>, 2014.
- Tyndall, G., Cox, R., Granier, C., Lesclaux, R., Moortgat, G., Pilling, M., Ravishankara, A., and Wallington, T.: Atmospheric chemistry of small organic peroxy radicals, *J. Geophys. Res.-Atmos.*, 106, 12157–12182, 2001.
- Villeneuve, E. and Lesclaux, R.: Kinetics of the cross reactions of CH_3O_2 and $\text{C}_2\text{H}_5\text{O}_2$ radicals with selected peroxy radicals, *J. Phys. Chem. C*, 100, 14372–14382, <https://doi.org/10.1021/jp960765m>, 1996.
- Wang, Y., Zhao, Y., Li, Z., Li, C., Yan, N., and Xiao, H.: Importance of hydroxyl radical chemistry in isoprene suppression of particle formation from α -pinene ozonolysis, *ACS Earth Space Chem.*, 5, 487–499, <https://doi.org/10.1021/acsearthspacechem.0c00294>, 2021.
- Wolfe, G. M., Marvin, M. R., Roberts, S. J., Travis, K. R., and Liao, J.: The Framework for 0-D Atmospheric Modeling (FOAM) v3.1, *Geosci. Model Dev.*, 9, 3309–3319, <https://doi.org/10.5194/gmd-9-3309-2016>, 2016.
- Xu, L., Møller, K. H., Crouse, J. D., Otkjær, R. V., Kjaergaard, H. G., and Wennberg, P. O.: Unimolecular reactions of peroxy radicals formed in the oxidation of α -pinene and β -pinene by hydroxyl radicals, *J. Phys. Chem. A*, 123, 1661–1674, <https://doi.org/10.1021/acs.jpca.8b11726>, 2019.
- Yao, M., Zhao, Y., Hu, M., Huang, D., and Yan, N.: Multi-phase reactions between secondary organic aerosol and sulfur dioxide: kinetics and contributions to sulfate formation and aerosol aging, *Environ. Sci. Tech. Let.*, 6, 768–774, <https://doi.org/10.1021/acs.estlett.9b00657>, 2019.
- Zhang, H., Yee, L. D., Lee, B. H., Curtis, M. P., Worton, D. R., Isaacman-VanWertz, G., Offenberg, J. H., Lewandowski, M., Kleindienst, T. E., and Beaver, M. R.: Monoterpenes are the largest source of summertime organic aerosol in the southeastern United States, *P. Natl. Acad. Sci. USA*, 115, 2038–2043, <https://doi.org/10.1073/pnas.1717513115>, 2018.
- Zhao, Y., Thornton, J. A., and Pye, H. O. T.: Quantitative constraints on autoxidation and dimer formation from direct probing of monoterpene-derived peroxy radical chemistry, *P. Natl. Acad. Sci. USA*, 115, 12142–12147, <https://doi.org/10.1073/pnas.1812147115>, 2018.
- Zhao, Y., Yao, M., Wang, Y. Q., Li, Z. Y., Wang, S. Y., Li, C. X., and Xiao, H. Y.: Acylperoxy Radicals as Key Intermediates in the Formation of Dimeric Compounds in α -Pinene Secondary Organic Aerosol, *Environ. Sci. Technol.*, 56, 14249–14261, <https://doi.org/10.1021/acs.est.2c02090>, 2022.
- Zhao, Z. X., Zhang, W., Alexander, T., Zhang, X., Martin, D. B. C., and Zhang, H. F.: Isolating α -Pinene Ozonolysis Pathways Reveals New Insights into Peroxy Radical Chemistry and Secondary Organic Aerosol Formation, *Environ. Sci. Technol.*, 55, 6700–6709, <https://doi.org/10.1021/acs.est.1c02107>, 2021.